BIOCHEMISTRY
including biophysical chemistry & molecular biology

Article

pubs.acs.org/biochemistry

A Rational Design Strategy for the Selective Activity Enhancement of a Molecular Chaperone toward a Target Substrate

Francesco A. Aprile, Pietro Sormanni, and Michele Vendruscolo*

Department of Chemistry, University of Cambridge, Cambridge CB2 1EW, U.K.

Supporting Information

ABSTRACT: Molecular chaperones facilitate the folding and assembly of proteins and inhibit their aberrant aggregation. They thus offer several opportunities for biomedical and biotechnological applications, as for example they can often prevent protein aggregation more effectively than other therapeutic molecules, including small molecules and antibodies. Here we present a method of designing molecular chaperones with enhanced activity against specific amyloidogenic substrates while leaving unaltered their functions toward other substrates. The method consists of grafting onto a molecular chaperone a peptide designed to bind specifically an epitope in the target substrate. We illustrate this strategy by describing Hsp70 variants with increased affinities for α-synuclein and Aβ42 but otherwise unaltered affinities for other substrates. These designed variants inhibit protein aggregation and disaggregate preformed fibrils significantly more effectively than wild-type Hsp70 indicating that the strategy presented here provides a possible route for tailoring rationally molecular chaperones for specific purposes.

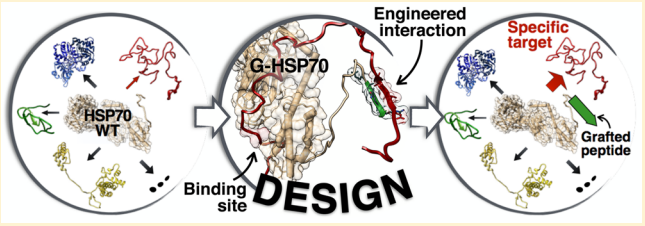

To function properly, most proteins should correctly fold into their native states, assemble into quaternary complexes and eventually be degraded and recycled, while avoiding uncontrolled aggregation.[1,2] Molecular chaperones, which are key components of the protein homeostasis system that maintains the integrity of the proteome,[3−7] assist essentially all of these processes by transiently associating with the proteins involved in them.[5−10] Given their remarkable efficiency in promoting folding and preventing aberrant interactions, major efforts have been focused on the development of strategies to harness the activity of molecular chaperones for biomedical and biotechnological applications.[11−21] Nevertheless, the complex network of interactions of these molecules[5−10] has made it difficult so far to fully exploit the opportunities that they offer.

A major emphasis is being placed in particular on the broad range of human disorders that arise from the failure of specific proteins to adopt or maintain their native conformations.[2−4,7,22−26] These pathological conditions, which are generally termed protein misfolding diseases,[2] are most commonly associated with the conversion of specific peptides or proteins from their soluble functional states into aberrant aggregates known as amyloid assemblies.[2−4,7,22−26] Although the detailed relationship between amyloid formation and pathology remains unclear, a growing body of evidence suggests that soluble oligomeric species formed during the formation of amyloid fibrils are particularly toxic, and that they are linked with the onset and progression of misfolding diseases.[23,27−29] The inhibition of protein aggregation therefore offers attractive modifying therapeutic strategies against these conditions.[3,22−24,30]

Among possible antiaggregation agents, molecular chaperones have attracted considerable interest, as they have been found to be effective in preventing the misfolding and aberrant assembly of many pathological proteins.[6−10] Compared to other molecules, such as small molecules and antibodies,[31,32] molecular chaperones show a much higher antiaggregation activity, being effective even at very low substoichiometric concentrations.[33−36] In particular, 70 kDa heat shock (Hsp70) proteins have been shown to play an essential role in preventing protein aggregation under both physiological and stress conditions,[6,37,38] and they have been found to be associated with amyloid deposits in the brains of patients with Alzheimer's, Parkinson's, and Huntington's diseases.[6,9] Overexpression of Hsp70 has also been found to reduce significantly amyloid-related toxicity in cellular[39,40] and animal[41,42] models.

Hsp70 consists of two structurally distinct domains connected by a linker - the nucleotide-binding domain with ATPase activity, which in *Homo sapiens* Hsp70 corresponds to residues 1−383, and the C-terminal substrate-binding domain, corresponding to residues 397−641. Two subdomains can be differentiated within the substrate-binding domain, a β-sandwich region (residues 397−507) named substrate-binding subdomain that contains the binding pocket and an α-helical subdomain (residues 508−641), named helical lid subdomain, which has been suggested to regulate the kinetics of substrate binding.[43] The helical lid subdomain comprises five α-helices and C-terminal intrinsically disordered region of 26 residues and has been proposed to act as a lid over the β-sandwich subdomain upon substrate binding.[44] The entire helical lid subdomain region has been shown to be highly

Received: April 26, 2015
Revised: July 15, 2015
Published: July 20, 2015

DOI: 10.1021/acs.biochem.5b00459
Biochemistry 2015, 54, 5103−5112

dynamic, and this behavior has been found to represent a prerequisite for Hsp70 to be able to accommodate a broad spectrum of client polypeptides into the binding pocket, including protein oligomers and aggregates.[45,46]

In vitro and *in vivo* approaches for potentiating or changing the activity of Hsp70 have been explored in recent years to provide new medical tools for neurodegenerative diseases.[11−21] Such methods are commonly based on the increase in the cellular levels of Hsp70[18−21,47] or on the stimulation of its ATPase activity with small molecules or nucleotide exchange factors to accelerate substrate turnover.[17,18] For example, the overexpression of Hsp70 has found important biotechnological applications, as the yield of poorly soluble proteins in prokaryotic or eukaryotic expression systems can be increased by co-expressing molecular chaperones.[47] Similarly, the stimulation of the ATPase functionality of Hsp70 has been recently proposed as a possible therapeutic strategy in the case of protein misfolding diseases, such as Alzheimer's and Parkinson's diseases.[18] These two approaches, however, involve a nonspecific stimulation of the molecular chaperone activities toward all possible natural substrates. Such nontargeted approaches can lead *in vivo* to an impairment of the cellular functions of the molecular chaperone, with potential pathological consequences, thus limiting their applicability.[13,48,49] Furthermore, the design of mutagenic variants with an engineered ATPase domain to characterize the mechanism of function of Hsp70 illustrated the difficulty of potentiating the activity of the molecular chaperone by the manipulation of its functional domains.[50,51]

Here we introduce a strategy for increasing by rational design the affinity of human Hsp70 for a specific substrate protein, without affecting its activity for other substrates. As a proof of principle, we apply this strategy to potentiate the binding and antiaggregation activity of Hsp70 against α-synuclein, a 140-residue protein whose aggregation is associated with Parkinson's disease. α-Synuclein is an intrinsically disordered protein, with an N-terminal region, corresponding to residues 1−60, involved in the binding and anchoring to the membrane,[52,53] a central region (residues 61−95), named the NAC region, that is hydrophobic and forms the core of the fibrils,[54] and an acidic C-terminal region. In this work, we have engineered two mutational variants of Hsp70 that retain the normal functions of the wild-type (wt) form but exhibit a higher affinity and antiaggregation activity selectively for α-synuclein, and an additional variant that possesses improved activity selectively for Aβ42, a 42-residue peptide closely associated with the onset and progression of Alzheimer's disease (Table 1).

MATERIALS AND METHODS

Protein Variants: Cloning, Expression, and Purification. The different complementary peptides were grafted at the C-terminal end of human Hsp70 (human Hsp70 1A, GenBank entry NP005336) by mutagenic polymerase chain reaction (PCR) with phosphorylated oligonucleotides. The A90C and 64P α-synuclein variants were obtained by mutagenic PCR of human wild-type α-synuclein (gi:80475099) using the QuikChange XLII kit (Qiagen, Venlo, Limburg, The Netherlands).

Recombinant N-hexa-His-tagged Hsp70 and all the mutant variants discussed here were overexpressed from the pET-28b vector (Merck KGaA, Darmstadt, Germany) in *Escherichia coli* BL21(DE3) Gold Strain (Agilent Technologies, Santa Clara, CA) and purified by affinity chromatography as previously described.[55] The monomeric fraction was in each case isolated by size exclusion chromatography using a Superdex 26/60 G75 column (GE Healthcare LifeSciences, Little Chalfont, U.K.). The thrombin cleavage efficiency, estimated by mass spectrometric analysis, was greater than 99% for all the variants, and the protein purity, as determined by sodium dodecyl sulfate−polyacrylamide gel electrophoresis (SDS−PAGE), exceeded 95%. The structural integrity of all the Hsp70 variants was assessed by far-ultraviolet (far-UV) circular dichroism (CD) spectroscopy at 25 °C (Figure S1 of the Supporting Information). All the grafted variants showed CD spectra compatible with the nativelike structure of the molecular chaperone. Protein concentrations were determined by absorbance measurements at 280 nm using theoretical extinction coefficients calculated with Expasy ProtParam.[56]

Human wild-type and mutant A90C and 64P α-synuclein variants were purified as previously reported.[28] The protein purity exceeded 95% as determined by SDS−PAGE analysis. The protein concentration was determined by absorbance measurement at 275 nm using an extinction coefficient of 5600 M^{-1} cm^{-1}.

Circular Dichroism. Far-UV CD spectra for all protein variants were recorded using a Jasco J-810 spectropolarimeter equipped with a Peltier holder, using a a 0.1 cm path length cuvette. Typically, samples contained 5 μM protein in 7 mM Tris buffer (pH 7.4) containing 170 mM KCl and 5 mM $MgCl_2$. The far-UV CD spectra of all the variants were recorded from 200 to 250 nm at 25 °C, and the spectrum of the buffer was systematically subtracted from the spectra of all protein samples.

Labeling Reaction. The A90C α-synuclein variant was labeled with DANSYL-MTS (Toronto research, Toronto, ON) via the cysteine thiol moiety. The protein was incubated in the presence of a 5 molar equivalent excess of the dye in PBS for 3 h at room temperature in the dark. The labeled protein was then purified from the excess of free dye with a P10 desalting column with the Sephadex G25 matrix (GE Healthcare LifeSciences, Little Chalfont, U.K.), divided into aliquots, flash-frozen, and stored at −80 °C. Each aliquot was thawed immediately prior to use. The labeling efficiency was >70% as estimated by mass spectrometry. The labeled protein concentration was estimated by absorbance measurement at 335 nm using the extinction coefficient of the free dye (4100 M^{-1} cm^{-1}).[57]

Substrate Binding to Hsp70 Variants. The interaction between the different Hsp70 variants and substrates was studied in 50 mM Tris buffer (pH 7.4) with 150 mM KCl and 5 mM $MgCl_2$ using fluorescence spectroscopy by titrating different concentrations of chaperone into a solution containing 2 μM dansyl-NR peptide (N-terminally labeled; Genemed Synthesis Inc., San Antonio, TX) or 2 μM dansyl α-synuclein after incubation of the mixtures for 1 h at 25 °C. The fluorescence emission spectrum of each sample was recorded from 400 to 630 nm after excitation at 330 nm, and the reported data correspond to the average intensity at the maximal emission wavelength of at least three different samples for which 10 spectra were recorded. The increase in the magnitude of the fluorescence signal was plotted as a function of molecular chaperone concentration and analyzed assuming a two-site or a single-site binding model to determine the fraction of Hsp70-bound ligand. Fluorescence titrations in the presence of *E. coli* protein extract were performed under the same conditions

DOI: 10.1021/acs.biochem.5b00459
Biochemistry 2015, 54, 5103−5112

described above at a crude extract concentration of 5 μM. The reported data correspond to the average fluorescence intensity at 520 nm of four different samples for which 10 spectra were recorded. The binding models used for fitting the data are described in the Supporting Information.

Crude extracts from nonexpressing *E. coli* BL21(DE3) Gold cells (Agilent Technologies) were obtained in a way similar to that used for extracts expressing human wild-type α-synuclein or Hsp70.

The fluorescence competition assay was performed on 10 μM Hsp70 wild type or GHsp70-NAC with 2 μM dansyl-NR peptide or dansyl-α-synuclein in the presence or absence of 2 μM α-synuclein wild type or 64P.

Luciferase Folding Assays. Refolding of chemically denatured firefly luciferase (Promega Corp., Madison, WI) by Hsp70 variants was conducted as described previously.[58] Briefly, luciferase (13 mg/mL) was diluted 42-fold into denaturation buffer [50 mM Tris (pH 7.4), 150 mM KCl, 5 mM $MgCl_2$, 6 M guanidinum hydrochloride, and 5 mM dithiothreitol]. The denaturation reaction was allowed to proceed for 40 min at 25 °C, and then a 1 μL aliquot was removed and mixed with 125 μL of refolding buffer [50 mM Tris (pH 7.4), 150 mM KCl, 5 mM $MgCl_2$, and 1 mM ATP] that was supplemented with the indicated chaperone proteins. Aliquots of 1 μL were then removed from the folding reaction mixtures and mixed with 60 μL of luciferase assay reagent (Promega Corp., Madison, WI). Luciferase activity was then measured with a CLARIOstar plate reader (BMG Labtech, Allmendgruen, Germany).

α-Synuclein and Aβ42 Aggregation Assays. Seeded aggregations of α-synuclein were performed at 70 μM protein in 50 mM Tris (pH 7.4), 150 mM KCl, 5 mM $MgCl_2$, and 20 μM ThT in the presence of 5% preformed fibrils at 37 °C in quiescence. Reaction mixtures were supplemented with different amounts of molecular chaperones. α-Synuclein fibrils were prepared as follows. Monomeric α-synuclein (70 μM) was incubated in 300 μL of 50 mM Tris (pH 7.4), 150 mM KCl, and 5 mM $MgCl_2$ (with 0.01% NaN_3 to prevent bacterial growth) at 37 °C while being constantly shaken at 200 rpm for 4 days. The fibrillar pellet was then centrifuged at 16000 **g** and washed twice with 300 μL of buffer. Fibrils were finally resuspended at a concentration of 100 μM and sonicated for 1 min, at 10% maximum power, with 30% cycles using a probe sonicator (Bandelin, Sonopuls HD 2070) to generate first-generation seeds. Second-generation fibrils were prepared by incubating 100 μM monomeric α-synuclein in the presence of 10 μM first-generation seeds (in terms of monomer concentration) in 500 μL of 50 mM Tris (pH 7.4), 150 mM KCl, 5 mM $MgCl_2$, and 0.01% NaN_3 at 37 °C under quiescent conditions for 13−14 h. The suspension was finally sonicated for 20 s, at 10% maximum power, with 30% cycles. Aβ42 aggregation assays were performed at 2 μM protein in 50 mM Tris (pH 7.4), 150 mM KCl, 5 mM $MgCl_2$, and 20 μM ThT at 37 °C in quiescence, in the absence or presence of a 1:200 (Hsp70:Aβ42) molar ratio of the chaperone variants. Emissions at 480 nm were recorded every 20 min, upon excitation at 440 nm, using a CLARIOstar plate reader (BMG Labtech, Allmendgruen, Germany). Plates were sealed to prevent evaporation.

Fibril Disaggregation Assay. α-Synuclein fibril solutions (10 μM), prepared as described in the previous section, were incubated overnight at 37 °C under quiescent conditions in the presence of Hsp70:α-synuclein molar ratios of 0, 1:20, 1:10, and 1:2 of wt Hsp70 and GHsp70-NAC. The samples were then centrifuged for 30 min at 16000 **g**, and 10 μL of the supernatant of each of the samples was analyzed by SDS−PAGE using 4 to 12% Bis-Tris NuPAGE gels (Life Technologies, Paisley, U.K.) in MES buffer under reducing conditions. Amounts of soluble α-synuclein and Hsp70 were estimated by densitometry analysis using Image-J (National Institutes of Health, Bethesda, MD).

RESULTS AND DISCUSSION

A Strategy of Grafting Complementary Peptides. The strategy that we present consists of the introduction into Hsp70 of an additional binding site for a specific epitope in a target protein (Figure 1). The purpose of this strategy is to selectively increase the affinity of Hsp70 for the target protein, while maintaining unaltered its affinity for other substrates. Given that most regions within the substrate-binding domain of Hsp70 have been shown to be essential for the substrate recognition process,[43] we engineered the additional binding site by appending a peptide designed to bind the target epitope at the C-terminus of the intrinsically disordered region of the helical lid subdomain (Figure 1b), which has recently been reported to interact with misfolded protein substrates.[59] The peptides that we graft, which are termed "complementary peptides", are designed using a recently introduced method,[62] which builds on related approaches aimed at modifying molecular scaffolds to target specific substrates.[60,61] In essence, this method identifies complementary peptides that bind with good specificity and affinity to disordered target regions of protein molecules using a fragment-and-join procedure starting from smaller peptides found to be interacting within β-strands in protein structures deposited in the Protein Data Bank (PDB) (see the Supporting Information).[62]

With this strategy, the Hsp70 variants that we designed retain the wild-type sequence but have an additional peptide, which binds to the target protein, grafted at the end of the disordered C-terminus of the molecular chaperone. As a result, the C-terminus of the engineered Hsp70 mutants effectively acts like a "fishing line", with a hook (the complementary peptide, colored green in Figure 1b) that selectively binds the specific epitope on the target protein, thus creating the "engineered interaction" shown in Figure 1b.

In this work, we illustrate this design strategy by engineering Hsp70 to specifically increase its activity toward α-synuclein (Figure 1). To this end, we engineered a grafted Hsp70 (GHsp70) variant with a complementary peptide designed to target the NAC region of α-synuclein and two additional GHsp70 variants that we use as controls: one with a complementary peptide designed to bind to the N-terminal region of α-synuclein and one with a complementary peptide designed to target the Aβ peptide (Table 1). We therefore generated three GHsp70 variants, GHsp70-NAC, GHsp70-N, and GHsp70-Aβ, designed for being specific to the NAC region of α-synuclein, the N-terminus of α-synuclein, and the Aβ peptide, respectively (Table 1).

Affinity and Specificity of GHsp70-NAC for Monomeric α-Synuclein. First, we evaluated the structural integrity of the grafted Hsp70 variants. All of them showed a CD spectrum compatible with the native-like structure of wild-type Hsp70 (Figure S1). Thus, we characterized the influence of the grafted peptide on the normal function of GHsp70-NAC. To this end, we characterized the ability of GHsp70-NAC to bind the NR peptide (NRLLLTG), which is frequently used as

DOI: 10.1021/acs.biochem.5b00459
Biochemistry 2015, 54, 5103−5112

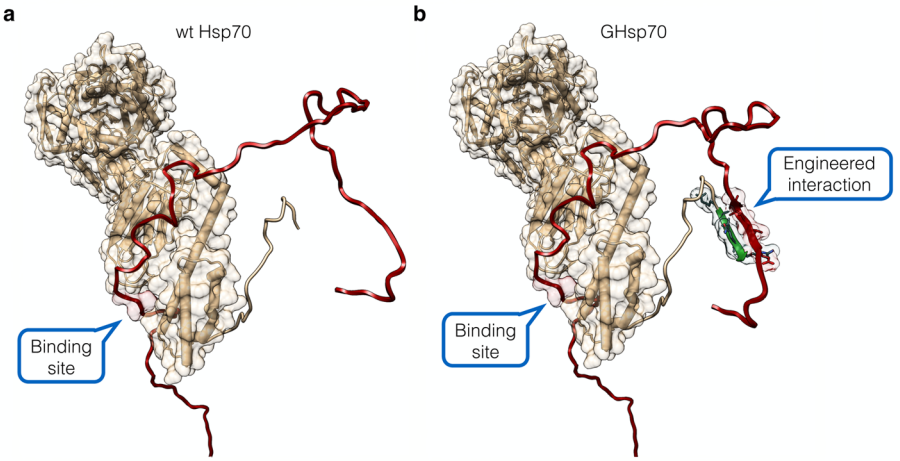

Figure 1. Illustration of the "fishing line" molecular chaperone rational design strategy. Cartoon representation of wild-type Hsp70 (wt Hsp70, panel a) and the grafted form (GHsp70) (b) bound to α-synuclein (colored red in both panels). The binding pocket of Hsp70 can accommodate a broad range of protein substrates, including α-synuclein at residues 71−82 (the "Binding site" in panels a and b). The strategy that we describe in this work is based on the engineering of an additional binding region in the disordered region of the α-helical subdomain, a result obtained by grafting a complementary peptide (colored green in panel b) at the end of the C-terminus of Hsp70. The new binding site (the "Engineered interaction" in panel b) is specific for an epitope on the target protein (the β-strand in α-synuclein is colored red in panel b, which is paired with the complementary peptide colored green). By this approach, we obtain the GHsp70 variant of Hsp70 with an increased affinity and specificity for α-synuclein (b). The structure of Hsp70 was adapted from PDB entry 2KHO.[65]

Table 1. Summary of the Three Designed Variants of Hsp70 Employed in This Work[a]

protein variant	complementary peptide	target sequence
GHsp70-NAC	EILVSYQ	EQVTNVG (α-synuclein residues 61−67)
GHsp70-N	RASVIQRV	KEGVVAAA (α-synuclein residues 12−20)
GHsp70-Aβ	FKLSVIT	QKLVFFA (Aβ42 residues 15−22)

[a]These variants (first column) target three specific epitopes (third column) in two different substrates (α-synuclein and Aβ42). The complementary peptides, which were grafted at the C-terminus (downstream from the EEVD sequence) of Hsp70 (see Figure 1), are also reported (second column).

a model substrate.[35,55] The NR peptide was N-terminally labeled with a dansyl fluorophore to allow the study of the formation
of its complex with GHsp70-NAC following the change in the fluorescence properties of the dansyl moiety upon titration of increasing quantities of the molecular chaperone. The normalized data were then fitted assuming a single-site binding model (see eq 1 of the Supporting Information). The titration experiments using the dansylated NR peptide yielded a binding curve for GHsp70-NAC that is undistinguishable from that of wild-type Hsp70 (Figure 2a), demonstrating that the design strategy does not alter the affinity of the molecular chaperone for the NR peptide (K_D = 10 μM).

In addition, we tested the ability of GHsp70-NAC to refold chemically denatured luciferase (see Materials and Methods). No significant difference between the grafted mutant and wild-type Hsp70 was observed (Figure 2b), showing that the GHsp70-NAC variant retains its refolding activity. These results indicate that our rational design procedure does not affect the allosteric regulation and functionality of Hsp70.

Taken together, these findings suggest that the grafting strategy that we describe in this work does not affect the binding and functionality of GHsp70-NAC. Thus, we sought to characterize the binding of GHsp70-NAC for monomeric α-synuclein with respect to wild-type Hsp70. We would expect that the insertion of an additional binding site specific for the NAC region of α-synuclein should increase the affinity for this substrate. To test this idea, we characterized the ability of the GHsp70-NAC variant to bind a labeled form of α-synuclein carrying at position 90 the dansyl fluorophore (dansyl-α-synuclein). We note that a dansyl group at this position should not significantly affect the binding, as the engineered peptide binds an epitope at positions 61−67, while the putative binding site of wild-type Hsp70 on α-synuclein has been mapped at positions 71−83.[35] The formation of the complex was studied by titrating increasing quantities of GHsp70-NAC into solutions containing dansyl-α-synuclein (Figure 2c), as described above for dansyl-NR. The results of the fluorescence titration experiment for GHsp70-NAC (Figure 2c) are better described assuming a two-site binding model rather than a single-site binding model (see Figure S2 and eqs 1 and 2 of the Supporting Information). Furthermore, the fitting yields a K_d for one of the two binding sites that is more than 1 order of magnitude lower than that obtained by fitting the fluorescence data of wild-type Hsp70 with a single-site binding model [from 40 μM of the wild type to ∼1 μM of GHsp70-NAC (Figure 2c)].

To further verify that the complementary peptide of GHsp70-NAC binds specifically the selected target sequence of α-synuclein, we generated an α-synuclein variant (α-synuclein-64P) with a proline residue inserted into the target sequence (EQVPTNVGG). If the binding occurs at this site, we expect the proline insertion to cause a significant

DOI: 10.1021/acs.biochem.5b00459
Biochemistry 2015, 54, 5103−5112

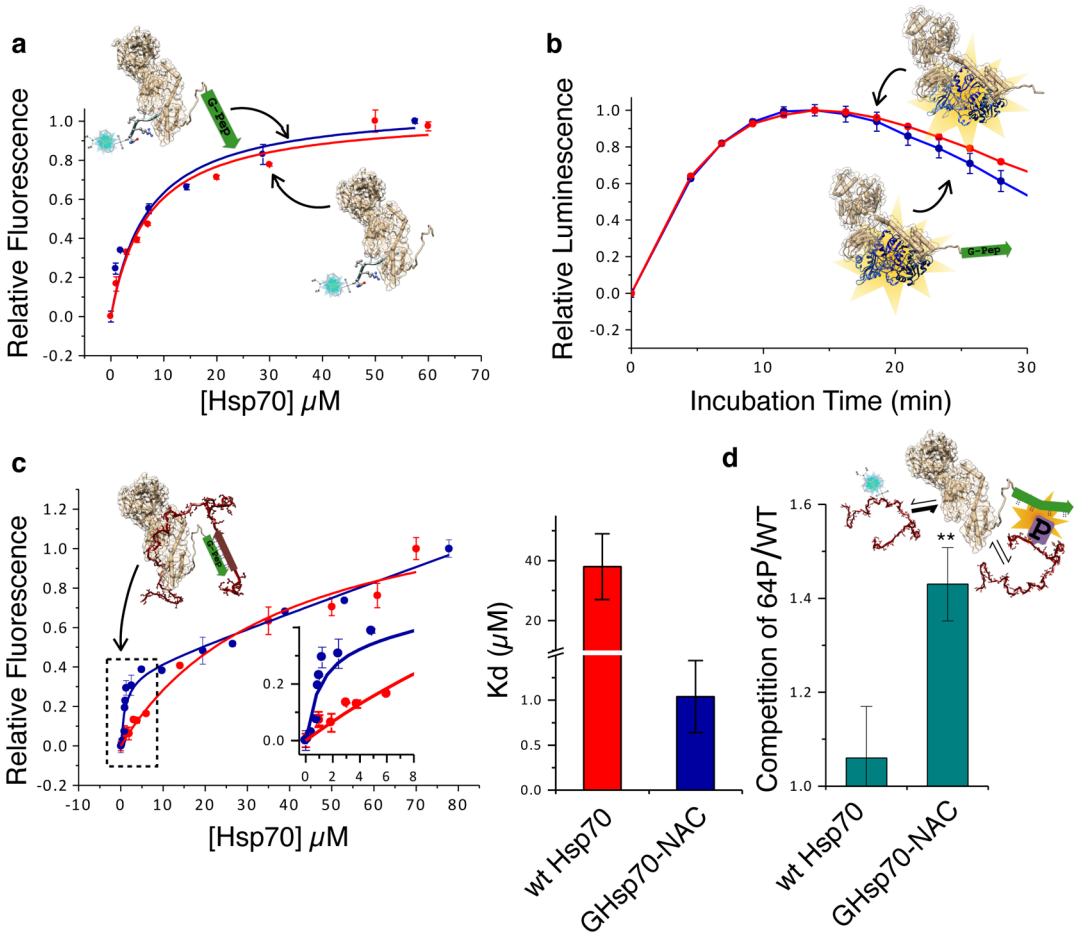

Figure 2. Grafted Hsp70 (GHsp70) variants retain normal binding and folding capability. (a) Fluorescence titration assays with 2 μM dansyl-NR of wild-type Hsp70 (red) and GHsp70-NAC (blue). Data were fitted with a single-site binding model (eq 1 in the Supporting Information). (b) Luciferase refolding assays of wild-type Hsp70 (red) and GHsp70-NAC (blue). Lines are guides for the eye. (c) Fluorescence titrations of wild-type Hsp70 (red) and GHsp70-NAC (blue) in the presence of 2 μM dansyl-α-synuclein. Fluorescence titration data of wild-type Hsp70 were fitted using a single-site binding model (eq 1 in the Supporting Information). Data of GHsp70-NAC were fitted with a two-site binding model (eq 2 of the Supporting Information). The bar plot shows the increased binding affinity of GHsp70-NAC ($K_d \sim 1$ μM) with respect to the wild type ($K_d \sim 40$ μM). (d) Fluorescence competition assays of 10 μM wild-type Hsp70 or GHsp70-NAC, incubated in the presence of 2 μM dansyl-α-synuclein. The decrease in fluorescence in the presence of 2 μM of α-synuclein wild type relative to the decrease in the presence of the same concentration of α-synuclein 64P is reported in the bar plot. Fluorescence data were processed using eq 3 in the Supporting Information. The statistical significance of the difference with the first column was assessed with a t test (**$p < 0.01$).

weakening of the interaction between the complementary peptide of GHsp70-NAC and α-synuclein. Thus, we performed fluorescence competition assays with wild-type Hsp70 or GHsp70-NAC in the presence of 2 μM dansyl-α-synuclein and 2 μM nonlabeled α-synuclein wild type or α-synuclein-64P (see Materials and Methods, Figure 2d, and eq 3 in the Supporting Information). The strength of the competition between dansyl-α-synuclein and the nonlabeled α-synuclein or α-synuclein-64P for the binding to the Hsp70 variants can be estimated from the decrease in fluorescence intensity, which is proportional to the amount of bound dansyl-α-synuclein, observed upon addition of nonlabeled α-synuclein variants to the solution. For wild-type Hsp70, we found that α-synuclein-64P was as efficient as wild-type α-synuclein in competing with dansyl-α-synuclein (Figure 2d). On the contrary, when GHsp70-NAC was present in solution, the competition of wild-type α-synuclein was ~1.4 fold stronger than that of α-synuclein-64P (Figure 2d). These results indicate that the proline insertion was able to largely disrupt the interaction between the complementary peptide and the target region of α-synuclein and, therefore suggest that the complementary peptide of GHsp70-NAC specifically binds the region of α-synuclein containing the target sequence. The residual capability of α-synuclein-64P to compete with dansyl-α-synuclein is likely related with the interaction with the binding pocket of the substrate-binding domain, which is the same in both wild-type Hsp70 and GHsp70-NAC.

To confirm the increased specificity of the GHsp70-NAC for α-synuclein, we performed fluorescence competition assays in the presence of binary and complex protein mixtures. First, we estimated the capability of α-synuclein to compete for the binding to GHsp70-NAC with the NR peptide. Having shown in Figure 2 that the affinities of binding of the NR peptide to wild type Hsp70 and to GHsp70-NAC are the same. Thus, solutions of 10 μM wild-type Hsp70 or GHsp70-NAC with 2 μM dansyl-NR peptide were incubated in the presence and absence of 2 μM nonlabeled α-synuclein as described in the previous paragraph (Figure 3a). Data were then analyzed as reported in the Supporting Information (eq 4). We found a statistically significant two-fold greater decrease of bound NR for GHsp70-NAC than for wild-type

DOI: 10.1021/acs.biochem.5b00459
Biochemistry 2015, 54, 5103−5112

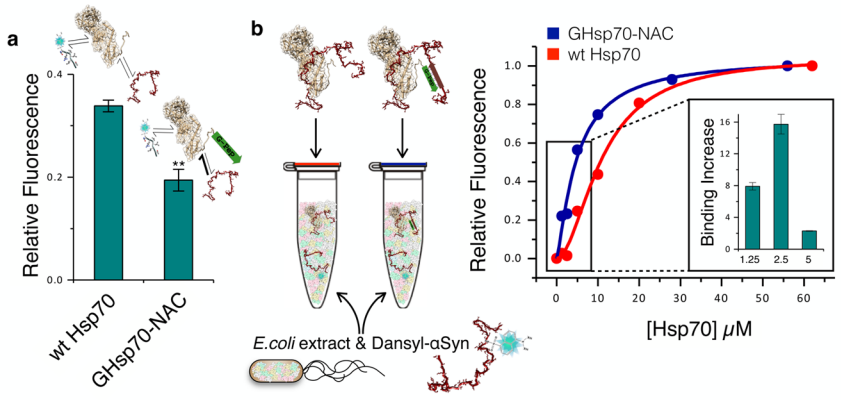

Figure 3. GHsp70-NAC shows a preferential binding for α-synuclein in binary and complex protein mixtures. (a) Fluorescence competition assay of wild-type Hsp70 and GHsp70-NAC, incubated in the presence of 2 μM dansyl-NR. The relative decrease in fluorescence upon addition of 2 μM α-synuclein wild type is reported (see eq 4 in the Supporting Information). (b) Fluorescence titrations of wild-type Hsp70 (red line) and GHsp70-NAC (blue line) in the presence of 2 μM dansyl-α-synuclein and 0.05 mg/mL protein lysate from *E. coli* cells; error bars over four replicates are smaller than data points. Given the complexity of the binding occurring in a heterogeneous protein mixture, lines are to guide the eye (see Supporting Information). The inset reports the ratios between the fluorescence intensities measured in the presence of GHsp70-NAC and in the presence of wild-type Hsp70 at concentrations of 1.25, 2.5, and 5 μM. These ratios represent the increase in the level of complex formation in the presence of GHsp70-NAC. In panel a, the statistical significance of the difference with the first column was assessed with a *t* test (**$p < 0.01$).

Hsp70, indicating a preferential binding of monomeric α-synuclein. As a further validation of the enhanced specific binding of GHsp70-NAC to α-synuclein, we performed fluorescence titration experiments, monitoring the binding of wild-type Hsp70 and GHsp70-NAC to dansyl-α-synuclein in the presence of 0.05 mg/mL cellular protein extract from *E. coli* (Figure 3b). This protein extract contains regulators of the Hsp70 chaperone activity, including ATP, ADP, and cochaperones, thus making the comparison more physiologically relevant, as well as many potential Hsp70 protein substrates, which can compete with dansyl-α-synuclein for the binding to the molecular chaperone. If our predicted binding mechanism for GHsp70-NAC is correct and the interaction with the grafted peptide is specific, we expect the cell lysate containing GHsp70-NAC to show a binding activity for dansyl-α-synuclein higher than that of the lysate containing wild-type Hsp70. In agreement with these expectations, we found that, particularly at low molecular chaperone concentrations (up to 5 μM), the interaction of dansyl-α-synuclein with GHsp70-NAC is significantly stronger than that with wild-type Hsp70. The analysis of the data indicates that at low concentrations (<3 μM), which are physiologically more relevant, GHsp70-NAC shows a capability of binding to α-synuclein ~1 order of magnitude higher than that of the wild-type molecular chaperone (Figure 3b, inset).

Finally, as a further validation, to confirm that the observed effect could specifically be attributed to the grafted peptide, and not to a generic extension of the C-terminus, we designed another GHsp70 variant. This new variant, called GHsp70-Aβ, carries at its C-terminus a peptide of the same length as that in GHsp70-NAC, but designed to bind to the Aβ peptide (Table 1). Also, in the case of the new GHsp70-Aβ variant, we observed a preferential binding for the target protein (Aβ42) with respect to wild-type Hsp70. In particular, we found that Aβ42 was able to compete with dansyl-NR better for the binding to GHsp70-Aβ than for the binding to wild-type Hsp70 and GHsp70-NAC (Figure S3). GHsp70-Aβ showed a binding affinity for α-synuclein similar to that of wild-type Hsp70 (Figure S4a), confirming that the generic insertion of a peptide does not produce nonspecific interactions with α-synuclein.

Overall, these data indicate that the complementary peptide grafted at the C-terminus of Hsp70 produces a specific increase in affinity for the target substrate.

Increased Antiaggregation Activity of the Designed Variants of Hsp70. In addition to their well-established role in assisting protein folding, it is increasingly being recognised that molecular chaperones are able to protect against other dysfunctional protein behavior, including the formation of amyloid fibrils.[6−10] Although the molecular basis of this inhibition is still to be fully clarified, it has been shown that the antiaggregation activity of Hsp70 is related to the capability of the binding pocket to accommodate a broad range of monomeric and aggregated protein species.[45,46] Because GHsp70-NAC has an affinity for α-synuclein higher than that of wild-type Hsp70, we investigated whether it might also show a stronger inhibitory effect on α-synuclein aggregation.

To test this idea, we performed experiments under conditions where nucleation events are bypassed by introducing a suitable amount (5%) of preformed seeds into the initial reactive mixture (see Materials and Methods).[63] Under these conditions, the soluble monomer consumption is mainly governed by elongation events. Thus, we performed seeded aggregation assays at increasing concentrations of wild-type Hsp70 or GHsp70-NAC (Figure 4a,b). We found a specific concentration-dependent effect of the Hsp70 variants on the elongation phase of α-synuclein aggregation. The inhibitory effect was stronger (from 2- to 5-fold) for GHsp70-NAC (Figure 4b,d). This finding is in agreement with the observation that the NAC region of α-synuclein represents the self-assembly interface for the amyloid aggregation process.[64] Therefore, the complementary peptide might be able to interfere with the elongation phase by binding to the NAC region and making it inaccessible for further fibril growth and assembly.

To further support this conclusion, we generated another GHsp70 variant against α-synuclein using a peptide predicted to bind the N-terminus [GHsp70-N (Table 1)], which is not in the core of the amyloid fibrils.[54] We found that GHsp70-N was able to inhibit the seeded aggregation of α-synuclein in a concentration-dependent manner and showed an activity higher

DOI: 10.1021/acs.biochem.5b00459
Biochemistry 2015, 54, 5103−5112

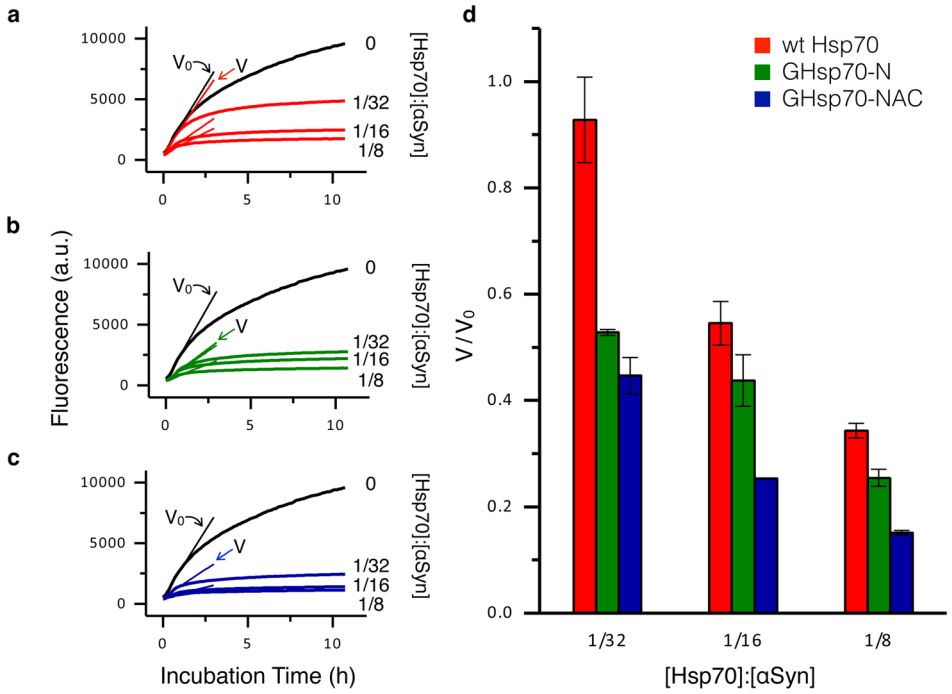

Figure 4. Inhibitory effects of two grafted Hsp70 (GHsp70-N and GHsp70-NAC) variants on α-synuclein aggregation. Seeded aggregation assays of α-synuclein in the absence (black line) and presence of 1:32, 1:16, and 1:8 molar ratios (Hsp70:α-synuclein) of wild-type Hsp70 (a, red), GHsp70-N (b, green), and GHsp70-NAC (c, blue). Dashed lines indicate the slope at time zero for the estimation of the maximal growth rate. (d) Reduction of the maximal growth rate upon titration of GHsp70 variants; data from panels a–c.

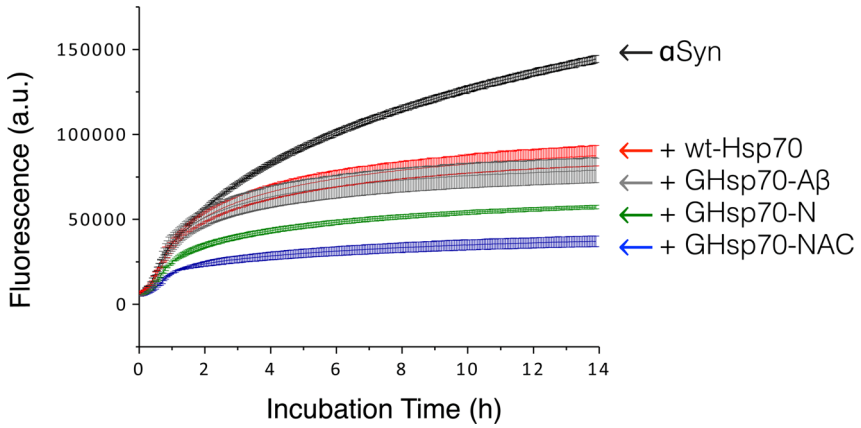

Figure 5. Specificity of the effects of grafted Hsp70 (GHsp70) variants on α-synuclein aggregation. Seeded aggregation assays of α-synuclein in the absence (black line) or presence of 2.3 μM wild-type Hsp70 (red), GHsp70-N (green), and GHsp70-NAC (blue). For comparison, the effect of GHsp70-Aβ (gray) is indistinguishable, within experimental error, from those of wild-type Hsp70 (red) and GHsp70-Aβ (gray).

than that of wild-type Hsp70 but significantly lower than that of GHsp70-NAC (Figure 4c,d). When compared to wild-type HSP70, GHsp70-N shows an increase in its affinity for monomeric α-synuclein similar to that observed for GHsp70-NAC (Figure S4b). We note, however, that the accuracy of the fluorescence titration data does not allow to reliably quantify changes in K_d values smaller than 1 order of magnitude. As a consequence, the weakened performance of GHsp70-N compared to that of GHsp70-NAC in inhibiting the aggregation of α-synuclein could simply reflect a slightly weaker binding affinity for monomeric α-synuclein, rather than the modulation of the elongation of the fibrils induced by the binding to the N-terminus or to the NAC region of the protein. In any case, these results show that the strength of the activity enhancement of the designed molecular chaperones can be modulated by targeting different regions of the target protein or by grafting different complementary peptides.

As a further test of specificity, we verified that the Hsp70 variant (GHsp70-Aβ) grafted to target Aβ inhibits α-synuclein aggregation in a way comparable to that of wild-type Hsp70 (Figure 5). Similarly, no significant increase in the inhibitory effect on Aβ42 aggregation was observed for the Hsp70 variants (GHsp70-NAC and GHsp70-N) grafted to target α-synuclein (Figure S5). By contrast, GHsp70-Aβ exhibits an enhanced ability to prevent Aβ aggregation (Figure S5).

We further observed that GHsp70-NAC not only has an effect in inhibiting the elongation of α-synuclein fibrils stronger than that of wild-type Hsp70 but also is better at binding and disaggregating them (Figure 6). We obtained these results by incubating α-synuclein fibrils in the presence of different

DOI: 10.1021/acs.biochem.5b00459
Biochemistry 2015, 54, 5103–5112

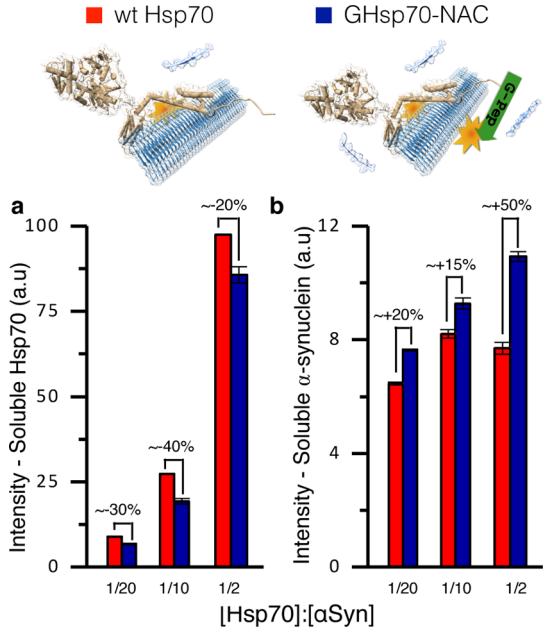

Figure 6. Increased binding and disaggregation effect on α-synuclein fibrils of GHsp70-NAC. Quantification by densitometry analysis from SDS−PAGE analysis of soluble Hsp70 (a) and soluble α-synuclein (b) in α-synuclein/fibril mixtures after overnight incubation in the presence of different ratios of wild-type Hsp70 (red) and GHsp70-NAC (blue). The intensities on the *y*-axis are derived from ImageJ software and are proportional to the amount of protein.

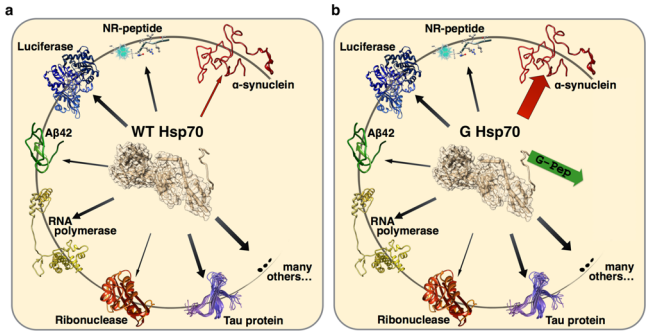

Figure 7. Scheme of our rational strategy for the selective enhancement of the activity of Hsp70 for a target protein. The grafted variant of Hsp70 described in this work (GHsp70-NAC) shows a selective increase in affinity for α-synuclein with respect to wild-type Hsp70, while leaving unaffected the affinity for its other substrates. The cartoon shows the network of interactions of wild-type (a) and grafted (b) Hsp70 variants with a pool of representative substrate proteins; the different affinities are indicated approximately by the different thicknesses of the arrows.

Hsp70:α-synuclein ratios of wild-type Hsp70 and GHsp70-NAC and by quantifying the amounts of molecular chaperone and α-synuclein present in the soluble fraction. We found that GHsp70-NAC is sequestered more efficiently by the α-synuclein fibrils and that it is able to disaggregate from α-synuclein mature fibrils more soluble species than wild-type Hsp70 (Figure 6 and Figure S6).

CONCLUSIONS

Using the case of Hsp70, we have presented a method of enhancing specifically the affinity and the antiaggregation activity of a molecular chaperone for a target protein. The results that we have obtained provide evidence that with the method that we have proposed it is possible to increase the activity of a molecular chaperone toward a specific substrate while maintaining unaffected its normal functionality for its other substrates (Figure 7).

ASSOCIATED CONTENT

Supporting Information

The Supporting Information is available free of charge on the ACS Publications website at DOI: 10.1021/acs.biochem.5b00459.

Supplementary methods and Supplementary Figures S1−S6 (PDF)

AUTHOR INFORMATION

Corresponding Author

*E-mail: mv245@cam.ac.uk.

Notes

The authors declare no competing financial interest.

REFERENCES

(1) Fersht, A. R. (1999) *Structure and Mechanism in Protein Science: A Guide to Enzyme Catalysis and Protein Folding*, W. H. Freeman, New York.

(2) Dobson, C. M. (2003) Protein folding and misfolding. *Nature 426*, 884−890.

(3) Balch, W. E., Morimoto, R. I., Dillin, A., and Kelly, J. W. (2008) Adapting proteostasis for disease intervention. *Science 319*, 916−919.

(4) Lindquist, S. L., and Kelly, J. W. (2011) Chemical and biological approaches for adapting proteostasis to ameliorate protein misfolding and aggregation diseases−progress and prognosis. *Cold Spring Harbor Perspect. Biol. 3*, a004507.

(5) Brehme, M., Voisine, C., Rolland, T., Wachi, S., Soper, J. H., Zhu, Y., Orton, K., Villella, A., Garza, D., and Vidal, M. (2014) A Chaperome Subnetwork Safeguards Proteostasis in Aging and Neurodegenerative Disease. *Cell Rep. 9*, 1135−1150.

(6) Hartl, F. U., Bracher, A., and Hayer-Hartl, M. (2011) Molecular chaperones in protein folding and proteostasis. *Nature 475*, 324−332.

(7) Hipp, M. S., Park, S.-H., and Hartl, F. U. (2014) Proteostasis impairment in protein-misfolding and-aggregation diseases. *Trends Cell Biol. 24*, 506−514.

(8) Hartl, F. U. (1996) Molecular chaperones in cellular protein folding. *Nature 381*, 571−580.

(9) Muchowski, P. J., and Wacker, J. L. (2005) Modulation of neurodegeneration by molecular chaperones. *Nat. Rev. Neurosci. 6*, 11−22.

(10) Bukau, B., Weissman, J., and Horwich, A. (2006) Molecular chaperones and protein quality control. *Cell 125*, 443−451.

(11) Morimoto, R. I., and Santoro, M. G. (1998) Stress-inducible responses and heat shock proteins: New pharmacologic targets for cytoprotection. *Nat. Biotechnol. 16*, 833−838.

(12) Evans, C. G., Chang, L., and Gestwicki, J. E. (2010) Heat shock protein 70 (hsp70) as an emerging drug target. *J. Med. Chem. 53*, 4585−4602.

(13) Whitesell, L., and Lindquist, S. L. (2005) HSP90 and the chaperoning of cancer. *Nat. Rev. Cancer 5*, 761−772.

(14) Sõti, C., Nagy, E., Giricz, Z., Vígh, L., Csermely, P., and Ferdinandy, P. (2005) Heat shock proteins as emerging therapeutic targets. *Br. J. Pharmacol. 146*, 769−780.

(15) Chaudhuri, T. K., and Paul, S. (2006) Protein-misfolding diseases and chaperone-based therapeutic approaches. *FEBS J. 273*, 1331−1349.

(16) Muchowski, P. J. (2002) Protein misfolding, amyloid formation, and neurodegeneration: a critical role for molecular chaperones? *Neuron 35*, 9−12.

(17) Brehmer, D., Rüdiger, S., Gässler, C. S., Klostermeier, D., Packschies, L., Reinstein, J., Mayer, M. P., and Bukau, B. (2001)

DOI: 10.1021/acs.biochem.5b00459
Biochemistry 2015, 54, 5103−5112

Tuning of chaperone activity of Hsp70 proteins by modulation of nucleotide exchange. *Nat. Struct. Biol. 8*, 427−432.
(18) Jinwal, U. K., John Koren, J. C., III, Leary, J. R. J., III, Abisambra, J. F., and Dickey, C. A. (2010) Hsp70 ATPase modulators as therapeutics for Alzheimer's and other neurodegenerative diseases. *Mol. Cell. Pharmacol. 2*, 43−46.
(19) Kalia, S., Kalia, L., and McLean, P. (2010) Molecular chaperones as rational drug targets for Parkinson's disease therapeutics. *CNS Neurol. Disord.: Drug Targets 9*, 741−753.
(20) Ebrahimi-Fakhari, D., Saidi, L.-J., and Wahlster, L. (2013) Molecular chaperones and protein folding as therapeutic targets in Parkinson's disease and other synucleinopathies. *Acta Neuropathol. Commun. 1*, 79.
(21) Jones, D. R., Moussaud, S., and McLean, P. (2014) Targeting heat shock proteins to modulate α-synuclein toxicity. *Ther. Adv. Neurol. Disord. 7*, 33−51.
(22) Ross, C. A., and Poirier, M. A. (2004) Protein aggregation and neurodegenerative disease. *Nat. Med. 10*, S10−S17.
(23) Haass, C., and Selkoe, D. J. (2007) Soluble protein oligomers in neurodegeneration: lessons from the Alzheimer's amyloid β-peptide. *Nat. Rev. Mol. Cell Biol. 8*, 101−112.
(24) Aguzzi, A., and O'Connor, T. (2010) Protein aggregation diseases: pathogenicity and therapeutic perspectives. *Nat. Rev. Drug Discovery 9*, 237−248.
(25) Tyedmers, J., Mogk, A., and Bukau, B. (2010) Cellular strategies for controlling protein aggregation. *Nat. Rev. Mol. Cell Biol. 11*, 777−788.
(26) Knowles, T. P., Vendruscolo, M., and Dobson, C. M. (2014) The amyloid state and its association with protein misfolding diseases. *Nat. Rev. Mol. Cell Biol. 15*, 384−396.
(27) Mannini, B., Mulvihill, E., Sgromo, C., Cascella, R., Khodarahmi, R., Ramazzotti, M., Dobson, C. M., Cecchi, C., and Chiti, F. (2014) Toxicity of protein oligomers is rationalized by a function combining size and surface hydrophobicity. *ACS Chem. Biol. 9*, 2309−2317.
(28) Cremades, N., Cohen, S. I., Deas, E., Abramov, A. Y., Chen, A. Y., Orte, A., Sandal, M., Clarke, R. W., Dunne, P., and Aprile, F. A. (2012) Direct observation of the interconversion of normal and toxic forms of α-synuclein. *Cell 149*, 1048−1059.
(29) Cohen, S. I., Linse, S., Luheshi, L. M., Hellstrand, E., White, D. A., Rajah, L., Otzen, D. E., Vendruscolo, M., Dobson, C. M., and Knowles, T. P. (2013) Proliferation of amyloid-β42 aggregates occurs through a secondary nucleation mechanism. *Proc. Natl. Acad. Sci. U. S. A. 110*, 9758−9763.
(30) Arosio, P., Vendruscolo, M., Dobson, C. M., and Knowles, T. P. (2014) Chemical kinetics for drug discovery to combat protein aggregation diseases. *Trends Pharmacol. Sci. 35*, 127−135.
(31) Solomon, B., Koppel, R., Hanan, E., and Katzav, T. (1996) Monoclonal antibodies inhibit in vitro fibrillar aggregation of the Alzheimer beta-amyloid peptide. *Proc. Natl. Acad. Sci. U. S. A. 93*, 452−455.
(32) Young, L. M., Saunders, J. C., Mahood, R. A., Revill, C. H., Foster, R. J., Tu, L.-H., Raleigh, D. P., Radford, S. E., and Ashcroft, A. E. (2014) Screening and classifying small-molecule inhibitors of amyloid formation using ion mobility spectrometry−mass spectrometry. *Nat. Chem. 7*, 73−81.
(33) Evans, C. G., Wisén, S., and Gestwicki, J. E. (2006) Heat shock proteins 70 and 90 inhibit early stages of amyloid β-(1−42) aggregation in vitro. *J. Biol. Chem. 281*, 33182−33191.
(34) Kumita, J. R., Poon, S., Caddy, G. L., Hagan, C. L., Dumoulin, M., Yerbury, J. J., Stewart, E. M., Robinson, C. V., Wilson, M. R., and Dobson, C. M. (2007) The extracellular chaperone clusterin potently inhibits human lysozyme amyloid formation by interacting with prefibrillar species. *J. Mol. Biol. 369*, 157−167.
(35) Roodveldt, C., Bertoncini, C. W., Andersson, A., van der Goot, A. T., Hsu, S. T., Fernández-Montesinos, R., de Jong, J., van Ham, T. J., Nollen, E. A., and Pozo, D. (2009) Chaperone proteostasis in Parkinson's disease: stabilization of the Hsp70/α-synuclein complex by Hip. *EMBO J. 28*, 3758−3770.
(36) Dedmon, M. M., Christodoulou, J., Wilson, M. R., and Dobson, C. M. (2005) Heat shock protein 70 inhibits α-synuclein fibril formation via preferential binding to prefibrillar species. *J. Biol. Chem. 280*, 14733−14740.
(37) Mayer, M., and Bukau, B. (2005) Hsp70 chaperones: cellular functions and molecular mechanism. *Cell. Mol. Life Sci. 62*, 670−684.
(38) Lu, T. Z., Quan, Y., and Feng, Z.-P. (2010) Multifaceted role of heat shock protein 70 in neurons. *Mol. Neurobiol. 42*, 114−123.
(39) Klucken, J., Shin, Y., Masliah, E., Hyman, B. T., and McLean, P. J. (2004) Hsp70 reduces α-synuclein aggregation and toxicity. *J. Biol. Chem. 279*, 25497−25502.
(40) Ran, R., Lu, A., Zhang, L., Tang, Y., Zhu, H., Xu, H., Feng, Y., Han, C., Zhou, G., and Rigby, A. C. (2004) Hsp70 promotes TNF-mediated apoptosis by binding IKKγ and impairing NF-κB survival signaling. *Genes Dev. 18*, 1466−1481.
(41) Cummings, C. J., Sun, Y., Opal, P., Antalffy, B., Mestril, R., Orr, H. T., Dillmann, W. H., and Zoghbi, H. Y. (2001) Over-expression of inducible HSP70 chaperone suppresses neuropathology and improves motor function in SCA1 mice. *Hum. Mol. Genet. 10*, 1511−1518.
(42) Auluck, P. K., Chan, H. E., Trojanowski, J. Q., Lee, V. M.-Y., and Bonini, N. M. (2002) Chaperone suppression of α-synuclein toxicity in a Drosophila model for Parkinson's disease. *Science 295*, 865−868.
(43) Mayer, M. P., Schröder, H., Rüdiger, S., Paal, K., Laufen, T., and Bukau, B. (2000) Multistep mechanism of substrate binding determines chaperone activity of Hsp70. *Nat. Struct. Biol. 7*, 586−593.
(44) Zhu, X., Zhao, X., Burkholder, W. F., Gragerov, A., Ogata, C. M., Gottesman, M. E., and Hendrickson, W. A. (1996) Structural analysis of substrate binding by the molecular chaperone DnaK. *Science 272*, 1606−1614.
(45) Schlecht, R., Erbse, A. H., Bukau, B., and Mayer, M. P. (2011) Mechanics of Hsp70 chaperones enables differential interaction with client proteins. *Nat. Struct. Mol. Biol. 18*, 345−351.
(46) Marcinowski, M., Höller, M., Feige, M. J., Baerend, D., Lamb, D. C., and Buchner, J. (2011) Substrate discrimination of the chaperone BiP by autonomous and cochaperone-regulated conformational transitions. *Nat. Struct. Mol. Biol. 18*, 150−158.
(47) Georgiou, G., and Valax, P. (1996) Expression of correctly folded proteins in Escherichia coli. *Curr. Opin. Biotechnol. 7*, 190−197.
(48) Nylandsted, J., Brand, K., and Jäättelä, M. (2000) Heat shock protein 70 is required for the survival of cancer cells. *Ann. N. Y. Acad. Sci. 926*, 122−125.
(49) Sherman, M., and Gabai, V. (2014) Hsp70 in cancer: back to the future. *Oncogene*, DOI: 10.1038/onc.2014.349.
(50) Montgomery, D. L., Morimoto, R. I., and Gierasch, L. M. (1999) Mutations in the substrate binding domain of the Escherichia coli 70 kDa molecular chaperone, DnaK, which alter substrate affinity or interdomain coupling. *J. Mol. Biol. 286*, 915−932.
(51) Vogel, M., Bukau, B., and Mayer, M. P. (2006) Allosteric regulation of Hsp70 chaperones by a proline switch. *Mol. Cell 21*, 359−367.
(52) Goedert, M. (2001) Alpha-synuclein and neurodegenerative diseases. *Nat. Rev. Neurosci. 2*, 492−501.
(53) Fusco, G., De Simone, A., Gopinath, T., Vostrikov, V., Vendruscolo, M., Dobson, C. M., and Veglia, G. (2014) Direct observation of the three regions in α-synuclein that determine its membrane-bound behaviour. *Nat. Commun. 5*, 3827.
(54) Vilar, M., Chou, H.-T., Lührs, T., Maji, S. K., Riek-Loher, D., Verel, R., Manning, G., Stahlberg, H., and Riek, R. (2008) The fold of α-synuclein fibrils. *Proc. Natl. Acad. Sci. U. S. A. 105*, 8637−8642.
(55) Aprile, F. A., Dhulesia, A., Stengel, F., Roodveldt, C., Benesch, J. L., Tortora, P., Robinson, C. V., Salvatella, X., Dobson, C. M., and Cremades, N. (2013) Hsp70 oligomerization is mediated by an interaction between the interdomain linker and the substrate-binding domain. *PLoS One 8*, e67961.
(56) Gill, S. C., and Von Hippel, P. H. (1989) Calculation of protein extinction coefficients from amino acid sequence data. *Anal. Biochem. 182*, 319−326.
(57) Gasymov, O. K., Abduragimov, A. R., and Glasgow, B. J. (2010) Excited protein states of human tear lipocalin for low-and high-affinity

DOI: 10.1021/acs.biochem.5b00459
Biochemistry 2015, 54, 5103−5112

ligand binding revealed by functional AB loop motion. *Biophys. Chem. 149*, 47−57.
(58) Lu, Z., and Cyr, D. M. (1998) Protein folding activity of Hsp70 is modified differentially by the hsp40 co-chaperones Sis1 and Ydj1. *J. Biol. Chem. 273*, 27824−27830.
(59) Smock, R. G., Blackburn, M. E., and Gierasch, L. M. (2011) Conserved, disordered C terminus of DnaK enhances cellular survival upon stress and DnaK in vitro chaperone activity. *J. Biol. Chem. 286*, 31821−31829.
(60) Ladiwala, A. R. A., Bhattacharya, M., Perchiacca, J. M., Cao, P., Raleigh, D. P., Abedini, A., Schmidt, A. M., Varkey, J., Langen, R., and Tessier, P. M. (2012) Rational design of potent domain antibody inhibitors of amyloid fibril assembly. *Proc. Natl. Acad. Sci. U. S. A. 109*, 19965−19970.
(61) Ganesan, A., Debulpaep, M., Wilkinson, H., Van Durme, J., De Baets, G., Jonckheere, W., Ramakers, M., Ivarsson, Y., Zimmermann, P., and Van Eldere, J. (2015) Selectivity of Aggregation-Determining Interactions. *J. Mol. Biol. 427*, 236−247.
(62) Sormanni, P., Aprile, F. A., and Vendruscolo, M. (2015) Rational design of antibodies targeting specific epitopes within intrinsically disordered proteins. *Proc. Natl. Acad. Sci. U.S.A.*, DOI: 10.1073/pnas.1422401112.
(63) Buell, A. K., Galvagnion, C., Gaspar, R., Sparr, E., Vendruscolo, M., Knowles, T. P., Linse, S., and Dobson, C. M. (2014) Solution conditions determine the relative importance of nucleation and growth processes in α-synuclein aggregation. *Proc. Natl. Acad. Sci. U. S. A. 111*, 7671−7676.
(64) Roodveldt, C., Andersson, A., De Genst, E. J., Labrador-Garrido, A., Buell, A. K., Dobson, C. M., Tartaglia, G. G., and Vendruscolo, M. (2012) A rationally designed six-residue swap generates comparability in the aggregation behavior of α-synuclein and β-synuclein. *Biochemistry 51*, 8771−8778.
(65) Bertelsen, E. B., Chang, L., Gestwicki, J. E., and Zuiderweg, E. R. (2009) Solution conformation of wild-type E. coli Hsp70 (DnaK) chaperone complexed with ADP and substrate. *Proc. Natl. Acad. Sci. U. S. A. 106*, 8471−8476.

DOI: 10.1021/acs.biochem.5b00459
Biochemistry 2015, 54, 5103−5112